Research Article

SOHAG JOURNAL OF SCIENCES

https://doi.org/10.21608/sjsci.2025.367748.1262

In-Silico Investigation of GRP78 Inhibition in Glioblastoma: Implications for Therapeutic Targeting

Mahmoud E. Rashwan[1,*], Mahrous R. Ahmed[1], and Abdo A. Elfiky[2]

[1] *Physics Department, Faculty of Science, Sohag University, Sohag, 82524, Egypt*
[2] *Biophysics Department, Faculty of Science, Cairo University, Giza, 12613, Egypt*
[*]*Email: mahmoud.ezz@science.sohag.edu.eg*

Received: 12th March 2025, **Revised:** 5th April 2025, **Accepted:** 29th April 2025
Published online: 23rd May 2025

Abstract: Glioblastoma (GBM) is an aggressive, fast-growing, and treatment-resistant tumor with high recurrence and poor prognosis. GRP78 is a molecular chaperone implicated in cancer cell survival, proliferation, and stress response, and overexpression has been shown to play a role in GBM development and drug resistance. In this work, we examine Zidovudine triphosphate (ZDV-TP) as a potential GRP78 inhibitor by computational approaches, including molecular docking, molecular dynamics (MD) simulations, and MMGBSA calculations. The results indicate that ZDV-TP securely binds to and energetically favors the ATP-binding site of GRP78, suggesting that it could disrupt its chaperone function. 100 ns MD simulations show that the GRP78-ZDV-TP complex is stable without significant conformational change, implying no destabilization of the protein structure. Such findings form a foundation that ZDV-TP is effective in inhibiting GRP78 and can abolish its role in GBM tumor formation and drug resistance. Further experimental proof should be tested for ZDV-TP to be an auspicious therapeutic target of GBM.
Keywords: GRP78, glioblastoma, molecular dynamics simulation, molecular docking, binding free energy calculation.

1. Introduction

Glucose-regulated protein 78, commonly known as HSPA5 or (immunoglobulin heavy chain binding protein, Bip), is one of the key members of the HSP70 family and is mainly located in the endoplasmic reticulum of eukaryotic cells. This multifunctional protein plays a vital role in maintaining cellular homeostasis by facilitating the proper folding and assembly of proteins, preventing the accumulation of misfolded proteins, and regulating the Unfolded Protein Response (UPR) [1, 2]. The UPR is an intracellular stress response that becomes engaged in response to an overwhelming number of unfolded or misfolded proteins within the lumen of the ER. This can be the result of a variety of cell stressors, such as hypoxia, nutrient deprivation, and oxidative stress [3].

In the cell, GRP78, or BiP, is an important molecular chaperone of the endoplasmic reticulum, maintaining correct protein folding and quality control. This process is intricately regulated through controlled hydrolysis of ATP, driven by the two functional domains: the N-terminal nucleotide-binding domain and the C-terminal substrate-binding domain of GRP78. Conformational shift by the binding of ATP to NBD converts GRP78 from an open ATP-bound state to a closed ADP-bound state, promoting substrate binding and subsequent folding. In its ATP-bound form, GRP78 has low substrate affinity, but upon hydrolysis of ATP to ADP, in the ADP-bound form, the GRP78 protein shows higher affinity for the substrate to stabilize unfolded or misfolded proteins during their folding process. This ATP-ADP cycle is vital for protein homeostasis to prevent aggregation [4–6]. While GRP78 is required for normal cellular function, its expression is often dysregulated in neoplastic tissues. A number of studies have documented that tumor cells hijack the cytoprotective functions of GRP78 to survive under hostile conditions in the tumor microenvironment and to develop resistance to therapeutic intervention [7, 8]. For instance, high levels of GRP78 have been reported in various malignancies, including breast cancer, pancreatic cancer, melanoma, and glioblastoma, associated with tumor progression in promoting cell survival and proliferation [1, 9, 10]. Glioblastoma or glioblastoma multiforme is a very malignant and aggressive brain cancer and is a WHO grade IV astrocytoma. It is the most common primary malignant central nervous system tumor and is responsible for approximately half of all CNS malignant tumors [11, 12]. Overexpression of GRP78 not only contributes to the adaptation of the cancer cells to stressors but also supports evasion from apoptosis-programmed cell death, which otherwise clears the damaged or dysfunctional cells from the body [13–15] .

Of the many roles of GRP78 in cancer, the most concerning is that it plays a role in enhancing resistance to chemotherapy and radiotherapy; GRP78, by modulating UPR, helps the cancer cells cope with cytotoxicity caused by these modes of treatment. Other works showed that downregulation of GRP78 could enhance the sensitivity of tumor cells to chemotherapy drugs such as doxorubicin and cisplatin [2, 14, 16] .The GRP78 induction is suggested to play an important role in the induction of angiogenesis-a process very crucial for tumor growth and metastasis-by regulating specific factors involved in neovascularization. It does so by interacting with numerous signaling pathways that trigger the proliferation and migration of endothelial cells [10, 13, 17].

Besides its established role in tumor biology, GRP78 has also been found to act as a receptor for various ligands associated with immune modulation and virus infection. For instance, GRP78 was recently described to function as a cell receptor for SARS-CoV-2, with very far-reaching implications for the care of cancer patients during virus pandemics [18]. This thus further underlines the intricacy of GRP78 functions in driving both tumorigenesis and whole patient health.

Since GRP78 has a great and significant role in promoting the survival of tumors and tumor resistance to drugs, potent inhibitors against this protein have been under urgent demand. Recently, it has been accentuated that some inhibitors can effectively compromise its protecting role and increase the sensibility of cancer cells to previously developed therapies. For instance, compounds like HA15 have shown great potential in the induction of apoptosis in lung cancer cells through the inhibition of GRP78 activity [19]. There are also natural products, such as genistein and epigallocatechin gallate, which exhibit a potential to decrease the expression or activity of GRP78 at pharmacological concentrations [20, 21]. The fact that GRP78 is exposed on the surface of tumor cells but not on normal tissues further justifies the possibility of targeted therapies against this protein and may provide the ability to selectively destroy malignant cells while sparing normal ones [13].

Zidovudine (ZDV-TP) was initially developed as an anticancer drug and later found effective against HIV in 1985 [22] . It was a synthetic analog of thymidine. Approved in 1990, zidovudine was the first antiretroviral agent approved for use in the treatment of HIV disease in children. Zidovudine must first be converted to its active form, Zidovudine-triphosphate (ZDV-TP), by intracellular phosphorylation by thymidylate and non-specific kinases. In this way, zidovudine triphosphate acts to inhibit HIV reverse transcriptase, terminate proviral DNA synthesis, and prevent viral replication. Being a member of the nucleoside reverse transcriptase inhibitor (NRTI) class of drugs, it has remained a mainstay of many HIV treatment regimens [23, 24]. ATP, ADP, and AMP are critically an intracellular molecule involved in energy transfer and signal transduction, mostly through protein phosphorylation, hence controlling cellular energy homeostasis. Since ZDV-TP, with its three phosphate groups similar to ATP, may interact with the nucleotide-binding domain of GRP78, it is of importance to investigate the potential interaction between ZDV-TP and GRP78, considering how this could affect the function of the protein and cellular energy dynamics [25, 26].

All these words reveal that, while GRP78 plays a critical role in the maintenance of protein homeostasis under physiological conditions, its dysregulation accounts for a major "dark side" in cancer pathology. The dual role of GRP78 as guardian of cellular integrity and facilitator of tumor survival points to its great potential as a target for therapy [9]. Further research into the mechanisms by which GRP78 supports tumor growth and treatment resistance may thus open new avenues for innovative strategies aimed at disrupting its protective roles in cancer cells. By understanding the multifaceted functions of GRP78 within the context of oncology, researchers hope to develop more effective therapies that can overcome the challenges posed by this enigmatic protein [27]. Utilizing the computational biophysical approach and using bioinformatics tools such as protein data bank (PDB) a website contains the solved structures of all proteins by x-ray diffraction or Nuclear magnetic resonance (NMR) or Cryogenic electron microscopy (cryo-EM), also PubChem a website contains the structures of the ligands (chemical compounds) [28, 29]. We further use protein-ligand docking which is a method used to investigate whether the suggested ligand makes good interaction with protein [30, 31]. Moreover, molecular dynamics simulation is widely used to ensure the interaction between the ligand and the protein by analyzing the resulted trajectory of the MDS [32]. So, we aim to find a new inhibitive activity for ZDV-TP to GRP78 protein in order to enhance the cancer therapeutics.

2. Materials and methods

2.1. Preparing materials

2.1.1. Protein Structure Preparation

The crystallography structure of GRP78 by X-ray was obtained from the Protein Data Bank [PDB ID: 7N1R] as reported at 2.03 Å resolution, which was released in 2022 [33]. Also ATP-bound state structure of GRP78 with PDB ID [5E84] was obtained to study the interaction between ATP and GRP78 [28, 34]. The protein structure was further prepared using PyMOL software for subsequent docking studies. In particular, all the water molecules, cofactors, ions, and ligands were removed, as were other chains, which means it only left the main chain of interest to be pursued. The cleaned PDB file was saved for later use in docking simulations.

2.1.2. Ligand Preparation

Ligand of interest was identified as Zidovudine-triphosphate (ZDV-TP), obtained from the PubChem database (https://pubchem.ncbi.nlm.nih.gov/compound/72187) with ID number (72187). The chemical structure of the ligand was optimized and minimized using Open Babel software, with the application of conjugate gradient method with the Universal Force Field (UFF) in order to ensure a stable conformation for docking [35] . Further, the minimized ligand structure was prepared for docking with the GRP78 protein.

2.2. Protein-ligand docking

The re-docking experiment was performed on GRP78 with the ligand co-crystallized (AMP) in the crystal structure PDB ID: 7N1R to validate the correctness of the docking protocol and resulted in -8.8 kcal/mol binding affinity. Subsequently, the Root-mean-square deviation (RMSD) was calculated between the re-docked ligand and its corresponding crystallographic pose. An RMSD value less than 2.0 Å was taken as acceptable and therefore representative of the reliability of the adopted docking procedure in reproducing the known binding mode of the ligand within the protein active site.

In doing so, the docking grid box was centered over the putative binding site of GRP78. For GRP78 with the center of the grid specified at coordinates (x: 67.88, y: -8.840, z: -1.12), setting up the grid box dimensions of 78 x 46 x 72 $Å^3$. which was considered big enough for the ligand to explore potential

binding modes within the protein's active site. Resolution was performed with a grid spacing of 0.375 Å to give high-resolution outcomes for the docking calculation. This grid box had been defined using Auto Dock Tools, allowing the proper fine-tuning of the space where the docking search took place and ensuring the capability for interaction of the ligand with key active residues in the GRP78 binding pocket [36, 37] .

Molecular docking simulations were performed using Auto Dock Vina software, one of the most powerful and widely used software tools due to its efficiency in computing putative protein- ligand interactions. A total of 9 docking poses for the ZDV-TP ligand were generated in this study to ensure diversity in possible binding configurations of the ligands. The exhaustiveness parameter, which defines the thoroughness of the search, was set to 32 [38] .

Full flexibility of the ligand was considered by enabling rotatable bonds, which will allow the ligand to assume multiple orientations and conformations during the docking process. Auto Dock Vina used a Monte Carlo search algorithm to explore the conformational space of the ligand and predict the optimal binding pose. The search algorithm iteratively sampled different ligand conformations and binding modes, evaluating each pose based on its predicted binding affinity. The final docking result was ranked according to the lowest binding affinity (ΔG), with the most favorable pose selected for further analysis.

The final docking poses were visualized using Auto Dock Tools and PyMOL software to study the interactions between the ZDV-TP ligand and the GRP78 protein [36, 39] . The interactions of the ligand with the specific key residues at the active site of the protein were closely monitored, taking into consideration hydrogen bonds, hydrophobic interactions, and electrostatic forces that are responsible for the stability of binding using the Protein-Ligand interaction profiler (PLIP) and Protein Plus webservers [40–42].

2.3. Molecular dynamics simulation

Further validation on the stability of ligand-protein interactions and to study the dynamic behavior of the complex, MDS was carried out. The initial structure of the ligand-protein complex was taken from the best docking pose produced through Auto Dock Vina. Input files were prepared through using the CHARMM-GUI web server for preparing the system into an MD simulation [43]. The protein alone and the protein-ligand complex was prepared by uploading the structure of the cleaned protein (no water or ligands) and the docked complex to the CHARMM-GUI web platform, where it was processed for solvation, ionization, and force field application. A water box was added around the complex to mimic the physiological environment, and then sodium (Na+) or chloride (Cl-) ions were added in order to neutralize the system and maintain physiological ionic strength with a concentration 0.154 mol/L [43] . The CHARMM36 force field was applied to the system, which is widely used for protein-ligand simulations due to its accuracy in describing macromolecular and small molecule interactions [44].

Using GROMACS, a molecular dynamics simulation software [45]. The two systems (protein and complex) were minimized for energy to get rid of some steric clashes or unnatural interactions introduced during the system's setup. The minimized systems were allowed to equilibrate under an NVT ensemble to stabilize the temperature using the V-rescale thermostat at 310.15 K with cut-off 12 Å, time constant of 0.1 ps and the integration time step was 1 fs. and then under NPT ensemble to achieve proper equilibration of pressure and density. Production MD simulations were performed under NPT ensemble after equilibration using C-rescale (stochastic cell rescaling) barostat at 310.15 K and 1 atm for 100 ns using the Langevin dynamics method to control the temperature and pressure. The integration time step was 2 fs, with a cut-off distance of 12 Å, time constant of 0.5 for the non-bonded interaction. The long-range electrostatic interactions were treated using the particle mesh Ewald (PME) method.

In this simulation, the stability of the protein-ligand interaction was pursued using the RMSD of the protein alone and the protein- ligand complex and also using the Root-mean-square fluctuation RMSF of crucial residues involved in the binding of the ligand to the protein. The trajectories were analyzed using VMD and PyMOL for visualization of the interactions and conformational changes of the ligand within the protein binding site [46].

2.4. Gibbs binding free energy

The Gibbs binding free energy calculation was executed on the trajectories of MD simulation using Gmx_MMPBSA software in order to predict the Gibbs binding free energy between the ligand and GRP78 [47]. This calculation combines molecular mechanics energy terms with solvation free energy components to yield the theoretical binding affinity for a given complex with the aim of estimating the stability and strength of the protein-ligand interaction.

The binding free energy has been calculated by the following equations:

$$\Delta G_{bind} = G_{complex} - (G_{receptor} + G_{ligand}) \quad (1)$$

$$\Delta G_{bind} = \Delta H - T\Delta S \approx \Delta E_{MM} + \Delta G_{soly} - T\Delta S \quad (2)$$

$$\Delta E_{MM} = \Delta E_{inter} + \Delta E_{electrostatic} + \Delta E_{vdw} \quad (3)$$

$$\Delta G_{solvation} = \Delta G_{GB} + \Delta G_{SA} \quad (4)$$

Where, $G_{complex}$ is the free energy of the entire receptor-ligand complex, $G_{receptor}$ is the free energy of the receptor alone and G_{ligand} is the free energy of the ligand alone.

ΔE_{MM} is the molecular mechanics energy of the complex that includes van der Waals, electrostatic, and bond (interaction) energies.

$T\Delta S$ is the entropy change, $\Delta G_{solvation}$ is the solvation free energy is divided into two terms:

ΔG_{GB} is the Polar solvation energy, which is determined by using the Generalized Born equation, and ΔG_{SA} is the non-polar solvation energy, estimated from solvent-accessible surface area (SASA).

MM-GBSA (Molecular Mechanics/Generalized Born Surface Area) calculations were performed for the last 50 ns of

the 100 ns MD simulation trajectory to ensure that proper sampling of the stable interactions between ligand and protein is taken into consideration. The MMPBSA.py script, integrated under Amber Tools, was employed to process trajectory files for the computation of binding free energy [48]. Energy components (ΔE_{MM}, ΔG_{GB}, and ΔG_{SA}) were extracted and averaged over selected frames from the trajectory in order to obtain the final value of $\Delta G_{binding}$.

Further, each energy component's contribution was calculated to obtain an idea about the relative importance of electrostatic, van der Waals, and solvation energies in the binding of the ligand with the protein.

3. Results and Discussion

3.1. Protein-Ligand docking

The docking results from AUTODOCK vina contained 9 modes for binding of ZDV-TP with GRP78 NBD (ATP pocket), the best score of binding affinity is (-10.4 kcal/mol) which indicates favorable interaction between the protein and the ligand, figure.1 clarifies the representation of the best pose.

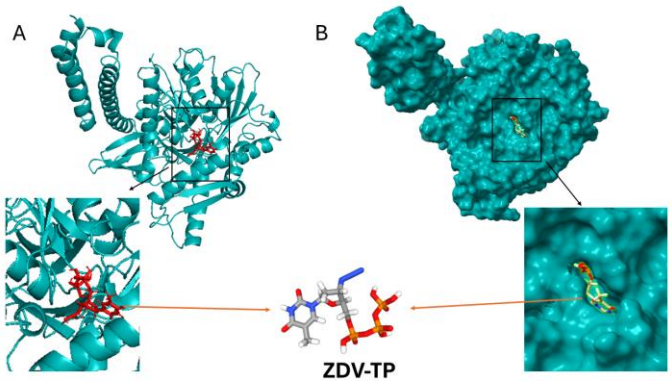

Figure 1: (A) cartoon representation of the GRP78-ZDVTP complex and (B) surface representation of the GRP78-ZDVTP complex

The GRP78-ATP PLIP analysis revealed 17 significant hydrogen bonds formed between the protein and the ligand as clarified in (Figure 2A)). Significant residues involved in hydrogen bonding are Asp34A (1 bond), Thr37A (3 bonds), Thr38A (1 bond), Tyr39A (1 bond), and Lys96A (1 bond) made

contact with oxygen and nitrogen atoms of ATP. A short residue region Gly226A, Gly227A, Gly228A, and Ala229A all contributed to ligand stabilizing with 1 bond, also Lys296A and Ser300A contributed with (1 bond) provided additional affinity. Notably, Gly364A was involved in 2 bonds, and Arg367A had 2 bonds through its guanidinium group, stabilizing ATP inside the binding pocket with crucial significance in GRP78's active site.

Also, the PLIP and protein plus webservers results show the type of interaction between ZDV-TP and the amino acids from GRP78 as shown in Table 1, Table 2 and Figure 2. The interaction between GRP78 and zidovudine triphosphate includes a series of significant hydrogen bonds, hydrophobic interactions, and salt bridges that collectively stabilize the complex. Notable hydrogen bonds include the interaction between residue (THR37) and ligand atom 9638 (O3), with a donor-acceptor distance of 3.02 Å and a donor angle of 145.19°. Another hydrogen bond is made by residue (TYR39) with the ligand atom 9635 (O3) at 3.87 Å with the donor angle of 134.04°. Further, the residue (LYS96) forms a hydrogen bond with the ligand atom 9638 (O3) at 2.61 Å, whereas residue (GLU201) interacts with the ligand atom 9639 (O3) at 2.99 Å and another bond with the ligand atom 9638 (O3) at 3.93 Å. More contributions are added through the glycine residues, where (GLY227) shows a bond at 3.00 Å distance to 9637 (O3) while (GLY228) contributes a contact to 9640 (O3) at 2.85 Å distance. Residue (THR229) also participates with two H-bonds-one ligand atom, 9640 (O3), and 3169 (O2)-at 2.99 and 3.89 Å distance, respectively.

The contribution of residue (GLU293) involves one hydrogen bond with the ligand atom 4235-O.co2 at 3.52 Å, while residue (LYS296) forms one bond with ligand atom 9644-O3 at 3.22 Å. Finally, residue (SER300) contributes two hydrogen bonds with ligand atom 9643-O3 at 2.96 Å and 2.41 Å, respectively. In addition to hydrogen bonding, another hydrophobic interaction occurred at the (ARG367) residue; here, the ligand atom 9629 and protein atom 5444 are 3.77 Å apart, suggesting a stabilizing nonpolar interaction. Besides, the complex is stabilized by salt bridges: (GLU256) and (ASP259) electrostatically interact with ZDV-TP at 4.11 Å and 5.37 Å distances, respectively, while (GLU293) also contributes a salt bridge at 3.15 Å.

Table 1: PLIP webserver analysis results show the hydrophobic interactions and salt bridges between GRP78 and ZDVTP.

NO.	Salt bridge			Hydrophobic Interactions		
	Amino Acid	Distance	Ligand Atoms	Amino Acid	Distance	Ligand Atoms
1	GLU256	4.11	9619	ARG367	3.77	9629
2	GLU259	5.37	9619			
3	GLU293	3.15	9619			

These combined hydrogen bonds, hydrophobic interactions, and salt bridges of GRP78-ZDV-TP complex compared to the interaction between GRP78 and ATP shows a similar hydrogen bonding interaction (15 bonds for ZDV-TP, 17 bonds for ATP). Also clarifies the importance of both polar and nonpolar forces in stabilizing the GRP78-ZDV-TP complex, contributing to the binding affinity and specificity of the interaction.

3.2. Molecular dynamics simulation

MD simulations provided dynamic stability and flexibility of the ligand-protein complex, confirming the reliability of the docking results and further providing evidence of the strength and stability of the ligand-protein interaction. As the systems of GRP78 and GRP78-ZDVTP were equilibrated along 100 ns. Figure 3 shows the stability of the root mean square deviation (RMSD) of both the protein and the protein-ligand complex around average value of 4.80 Å and 4.73 Å respectively. As the values of RMSD were nearly the same this means the protein (GRP78) is stable during the interaction with the ligand (ZDV-TP). Also Figure 4 clarifies the root mean square fluctuations (per-residue RMSF) of GRP78 and GRP78-ZDVTP as it was the

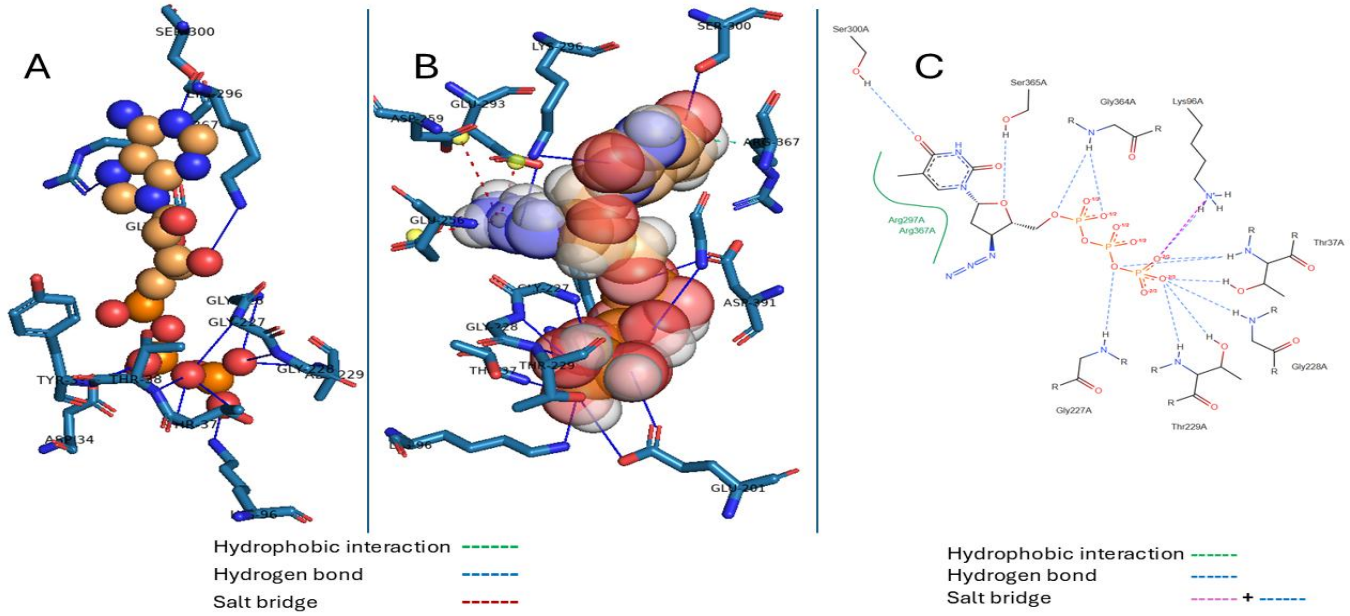

Figure 2: (A) PLIP webserver results, GRP78 interacted amino acids (blue - sticks) with ATP (spheres). (B) GRP78 interacted amino acids (blue - sticks) with ZDV-TP (spheres). (C) protein plus webserver results, the diagram shows the interactions between GRP78 and ZDV-TP.

same along the simulation. Only the two terminals of the protein fluctuated and that's due to the flexibility of these terminals is more than the core of structure of the protein, also residues (200-400) slightly fluctuate less in the complex than the protein due to the interaction between the ligand and the protein. This means that there is no conformational change of the protein structure due to the binding of ZDV-TP with GRP78, and the structure was not altered by ZDV-TP binding.

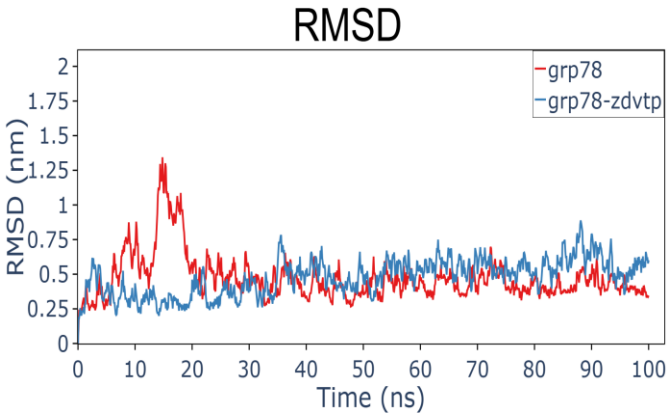

Figure 3: Root-mean-square deviation (RMSD) for protein and complex. GRP78 (red), GRP78-ZDVTP (blue).

The combination of the radius of gyration (RoG) and solvent accessible surface area (SASA) analysis showed the stability of the protein and the complex. The RoG was around 3 nm and the SASA was slightly above 300 nm^2 for GRP78 and GRP78-ZDVTP as in figure 5 and figure 6 and proves that the structure and the folding state of the protein wasn't affected by the binding of the ligand.

Table 2: PLIP webserver analysis results, show the formed Hydrogen bonds between GRP78 and ZDVTP.

NO.	Hydrogen bond					
	Amino Acid	Distance H-A	Distance D-A	Donor Angle	Donor Atom	Acceptor Atom
1	THR37	2.13	3.02	145.19	174 [Nam]	9638[O3]
2	TYR39	3.09	3.87	134.04	202 [Nam]	9635[O3]
3	LYS96	1.60	2.61	170.52	1078 [N3+]	9638[O3]
4	GLU201	2.61	2.99	103.12	9639 [O3]	2767[O3]
5	GLU201	3.00	3.93	163.22	9638 [O3]	2768[O-]
6	GLY227	1.99	3.00	169.40	3152 [Nam]	9637[O3]
7	GLY228	1.88	2.85	157.41	3159 [Nam]	9640[O3]
8	THR229	2.19	2.99	133.73	3166 [Nam]	9640[O3]
9	THR229	3.11	3.89	138.00	9640 [O3]	3169[O2]
10	GLU293	2.62	3.52	147.87	9618 [N3]	4235 [O.co2]
11	LYS296	2.61	3.22	118.26	4282 [N3+]	9644[O3]
12	SER300	2.10	2.96	150.29	4354 [O3]	9643[O3]
13	SER300	2.41	2.96	115.41	9643 [O3]	4354[O3]
14	GLY364	2.93	3.86	151.66	5408 [Nam]	9641[O3]
15	ASP391	2.52	3.05	113.69	9642 [O3]	5851 [O.co2]

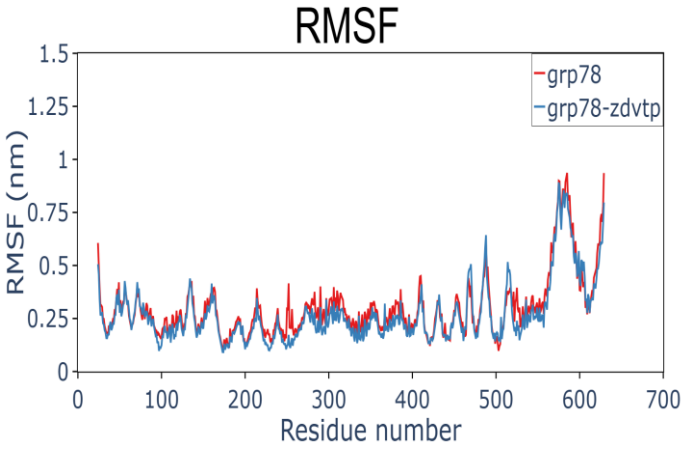

Figure 4: Root-mean-square fluctuation (RMSF) for protein and complex. GRP78 (red), GRP78-ZDVTP (blue).

As well as the number of hydrogen bonds analysis during the simulation displays ZDV-TP and GRP78 exhibit hydrogen bonds in between, and that's despite of the number of bonds was that the number of bonds not exceeded 10 while PLIP showed 15 bonds and that's due to PLIP doing static prediction but MDS calculation is more dynamic, reliable and depend on the dynamic interaction between protein and ligand, in which atoms is more flexible to move during time , as in figure 7.

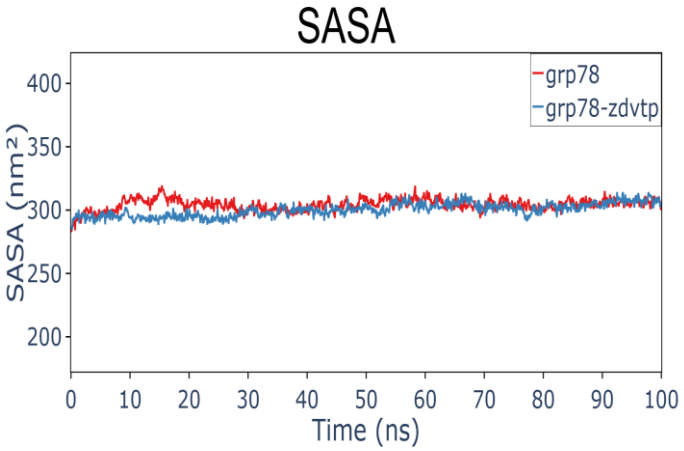

Figure 5: Surface accessible surface area (SASA) for protein and complex. GRP78 (red), GRP78-ZDVTP (blue).

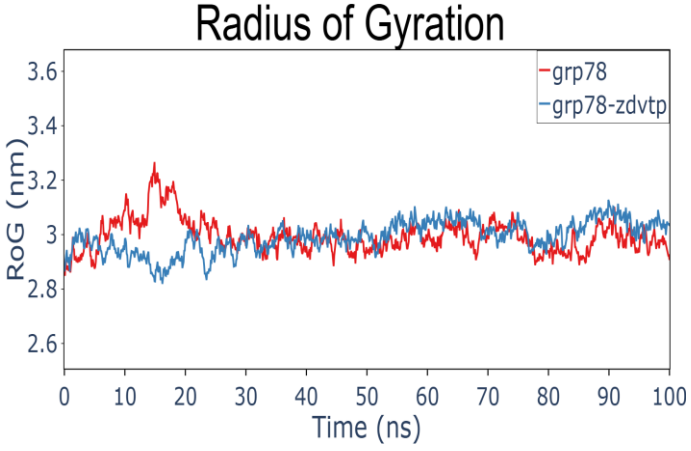

Figure 6: Radius of Gyration (RoG) for protein and complex. GRP78 (red), GRP78-ZDVTP (blue).

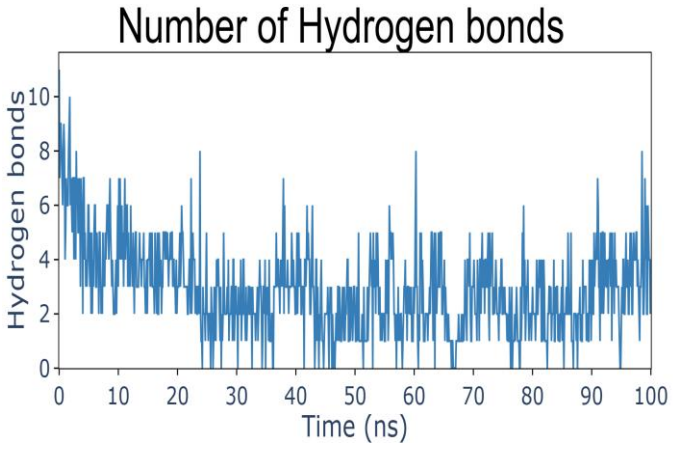

Figure 7: Hydrogen bonds between GRP78 and ZDV-TP

All these results indicate that the interaction between ZDV-TP and GRP78 ATP binding site is stable, and that ZDV-TP can prevent ATP binding which causes the interaction of GRP78 with other factors in the cell and inhibit the cancerous supportive behavior of GRP78.

3.3. Gibbs binding free energy

The MMGBSA calculations for the GRP78-ZDVTP complex were summarized in Table 3. The binding free energy components of the complex, receptor, and ligand are indicated, along with delta (Δ) values for complex minus receptor-ligand systems[49, 50]. The total free energy of the complex system was -11,699.46 kcal/mol, indicating a highly favorable interaction between the protein and the ligand. Notably, the electrostatic energy (EEL) of the complex was very negative (-38,961.96 kcal/mol), showing significant attractive forces between the charged residues of the receptor (GRP78) and the negatively charged ZDVTP. Similarly, the van der Waals energy (VDWaals) contribution was also very negative for the complex (-4,033.34 kcal/mol), suggesting that hydrophobic interactions are a dominant factor in the binding stability of the GRP78-ZDVTP. The isolated ligand (ZDVTP) provided a much lower total free energy of -89.02 kcal/mol with hardly any electrostatic contribution and a little van der Waals interaction in line with the assumption that the ligand itself does not bind strongly to itself at the receptor's binding site. For the isolated receptor (GRP78), though, a similarly low value of approximately -11,584.67 kcal/mol for total free energy is uncovered, showing how much the contribution of the ligand to binding affinity is crucial.

The Δ values (Complex - Receptor - Ligand) were most informative, with the ΔEEL value indicating a reduction in electrostatic interactions between the complex and its receptor-ligand components (-28.25 kcal/mol). The ΔVDWaals value of -38.50 kcal/mol suggests a marginal increase in hydrophobic interactions in the bound state, further stabilizing the complex. These results support that the interaction of GRP78 and ZDVTP is predominantly controlled by favorable electrostatic and van der Waals interactions, which contribute significantly to the binding free energy. The overall stability of the complex is proven by the negative binding free energy (-25.76 kcal/mol) with large magnitudes and by cooperative interactions of the

protein and the ligand. These calculations provided insights into the thermodynamic feasibility of the ligand binding to GRP78, further giving validation to the predicted binding affinity.

Table 3: The MM-GBSA calculations for the complex (GRP78-ZDVTP) after 100 ns Molecular dynamics simulation. Van der Waals Energy, Electrostatic Energy, Generalized Born, Solvent Accessible Surface Area Energy, Solvation Free Energy, and Total Free Energy Change components are listed.

Energy Component (kcal/mol)	Complex Average	Receptor Average	Ligand Average	Delta (Complex - Receptor - Ligand) Average
BOND	2007.16	1995.84	11.33	-0.00
ANGLE	4847.11	4796.31	50.80	0.00
DIHED	5822.64	5779.91	42.73	-0.00
VDWAALS	-4033.34	-3988.92	-5.92	-38.50
EEL	-38961.96	-39059.37	125.66	-28.25
EGB	-9398.97	-9417.55	-28.05	46.63
ESURF	254.32	255.63	4.33	-5.64
GGAS	-2554.81	-2422.75	-65.30	-66.76
GSOLV	-9144.65	-9161.92	-23.72	40.99
TOTAL	-11699.46	-11584.67	-89.02	-25.76

4. Conclusion

Glioblastoma (GBM) remains one of the most aggressive and treatment-resistant cancer forms, characterized by rapid tumor growth, high recurrence rates, and resistance to current treatment. Despite the clinical advances in surgery and chemotherapy treatments, therapy remains not very specific, and new methods of therapy are urgently needed. GRP78, a molecular chaperone in normal cells, also is involved in survival, growth, and stress response in cancer cells, is an excellent therapeutic target. Through inhibition of GRP78, it may be possible to disrupt vital cellular functions facilitating cancer progression and drug resistance.

In this study, we investigated Zidovudine triphosphate (ZDV-TP) as a potential GRP78 inhibitor by employing computer techniques like molecular docking, molecular dynamics (MD) simulation, and MMGBSA calculations. Molecular docking analysis revealed that ZDV-TP significantly interacted with GRP78 ATP-binding site in an energetically favorable manner, signifying tight and stable binding. The findings were further supported by MMGBSA calculations recognizing ZDV-TP binding to GRP78 to be energy-favorable and likely interfere with GRP78's chaperone activity.

The MD simulations for 100 ns showed that the GRP78-ZDV-TP complex was stable during the simulation. The RMSD and RMSF analyses verified that GRP78 maintained its structural integrity during the interaction with ZDV-TP without any remarkable conformational changes. In addition, the radius of gyration (RoG), solvent-accessible surface area (SASA) and number of hydrogen bonds analysis also favored the stability of the complex, indicating that the binding of ZDV-TP does not have an effect on the overall protein structure but may alter its functional dynamics.

These results show that ZDV-TP is a potent inhibitor of GRP78, blocking its binding to other cellular factors involved in tumor growth. By disrupting the chaperone function of GRP78, ZDV-TP has the potential to suppress the viability and proliferation of GBM cells, offering a novel approach to the therapy of glioblastoma. As a basis for the promising results of our computational studies, we propose experimental validation in vitro and in vivo to establish if ZDV-TP is truly a therapeutic agent. In addition, it is suggested that future research endeavors seek to elucidate the specific mechanism of action of ZDV-TP in GBM cells, assess its potential impact on GBM proliferation, and assess its combination with existing treatment strategies. This drug can enhance the treatment of GBM patients and potentially be usable in treatment of other cancers where GRP78 is essential for tumor proliferation and drug resistance.

CRediT authorship contribution statement:

"Conceptualization, M.E.R. and A.A.E.; methodology, A.A.E and M.E.R.; software, M.E.R.; validation, A.A.E. and M.E.R.; formal analysis, M.E.R.; investigation, A.A.E. and M.E.R.; resources, M.E.R.; data curation, M.E.R.; writing—original draft preparation, M.E.R.; writing—review and editing, M.E.R. , A.A.E. and M.R.A; visualization, M.E.R.; supervision, A.A.E. and M.R.A.; project administration, A.A.E. and M.R.A.; All authors have read and agreed to the published version of the manuscript."

Data availability statement

The data used to support the findings of this study are available from the corresponding author upon request.

Declaration of competing interest

The authors declare that they have no known competing financial interests or personal relationships that could have appeared to influence the work reported in this paper.

Acknowledgments

We acknowledge Bibliotheca Alexandrina for providing the HPC for the MDS calculations.

References

[1] J. Chen, E.G. Lynn, T.R. Yousof, H. Sharma, M.E. MacDonald, J.H. Byun, B. Shayegan, R.C. Austin, *Biomedicines*, 10 (2022) 1098.
[2] A.S. Lee, *Cancer Research*, 67 (2007) 3496–3499.
[3] A.A. Elfiky, A.M. Baghdady, S.A. Ali, M.I. Ahmed, *Life Sciences*, 260 (2020) 118317.
[4] Y. Liu, J. Chen, X. Li, X. Zhou, Y. Hu, S. Chu, Y. Peng, N. Chen, *CNS Neuroscience & Therapeutics*, 25 (2019) 899–910.
[5] J. Yang, M. Nune, Y. Zong, L. Zhou, Q. Liu, *Structure*, 23 (2015) 2191–2203.
[6] E. Dolgin, *Nature*, 597 (2021) 606–607.
[7] J. Li, A. Lee, *Current Molecular Medicine*, 6 (2006) 45–54.
[8] M. Farshbaf, A.Y. Khosroushahi, S. Mojarad-Jabali, A. Zarebkohan, H. Valizadeh, P.R. Walker, *Journal of Controlled Release*, 328 (2020) 932–941.

[9] Amos Olalekan Akinyemi, K. Simpson, Sunday Faith Oyelere, M. Nur, C.M. Ngule, C. Dayo, Vivian Adiila Ayarick, Felix Femi Oyelami, Oluwafunminiyi Obaleye, Dave-Preston Esoe, X. Liu, Z. Li, *Molecular Medicine*, 29 (2023).
[10] D.Y.A. Dadey, V. Kapoor, K. Hoye, A. Khudanyan, A. Collins, D. Thotala, D.E. Hallahan, *Clinical Cancer Research*, 23 (2017) 2556–2564.
[11] S. Grochans, A.M. Cybulska, D. Simińska, J. Korbecki, K. Kojder, D. Chlubek, I. Baranowska-Bosiacka, *Cancers*, 14 (2022) 1–32.
[12] M. Davis, *Clinical Journal of Oncology Nursing*, 20 (2016) 2–8.
[13] Rajalakshmi Amaresan, U. Gopal, *Cancer Cell International*, 23 (2023).
[14] R. Yerushalmi, A. Raiter, K. Nalbandyan, B. Hardy, *Oncology Letters*, 10 (2015) 2149–2155.
[15] Y. Fu, S. Wey, M. Wang, R. Ye, C.-P. Liao, P. Roy-Burman, A.S. Lee, *Proceedings of the National Academy of Sciences*, 105 (2008) 19444–19449.
[16] C. Bailly, M.J. Waring, *Biochemical Pharmacology*, 163 (2019) 269–278.
[17] G. Shani, W.H. Fischer, N.J. Justice, J.A. Kelber, W. Vale, P.C. Gray, *Molecular and Cellular Biology*, 28 (2008) 666–677.
[18] J. Shin, S. Toyoda, A. Fukuhara, I. Shimomura, *Biomedicines*, 10 (2022) 1995.
[19] J. Wu, Y. Wu, X. Lian, *Biology Open*, 9 (2020).
[20] S.P. Ermakova, B.S. Kang, B.Y. Choi, H.S. Choi, T.F. Schuster, W.-Y. Ma, A.M. Bode, Z. Dong, *Cancer Research*, 66 (2006) 9260–9269.
[21] X. Zhang, K.L. Cook, A. Warri, I.M. Cruz, M. Rosim, J. Riskin, W. Helferich, D. Doerge, R. Clarke, L. Hilakivi-Clarke, *Clinical Cancer Research*, 23 (2017) 814–824.
[22] R.E. McKinney, M.A. Maha, E.M. Connor, J. Feinberg, G.B. Scott, M. Wulfsohn, K. McIntosh, W. Borkowsky, J.F. Modlin, P. Weintrub, K. O'Donnell, R.D. Gelber, G.K. Rogers, S.N. Lehrman, C.M. Wilfert, *New England Journal of Medicine*, 324 (1991) 1018–1025.
[23] L. Mu, R. Zhou, F. Tang, X. Liu, S. Li, F. Xie, X. Xie, J. Peng, P. Yu, *Acta Pharmaceutica Sinica B*, 6 (2015) 158–162.
[24] N. Bhana, D. Ormrod, C.M. Perry, D.P. Figgitt, *Pediatric Drugs*, 4 (2002) 515–553.
[25] G. Haskó, J. Linden, B. Cronstein, P. Pacher, *Nature Reviews. Drug Discovery*, 7 (2008) 759–770.
[26] M. Garcia-Gil, M. Camici, S. Allegrini, R. Pesi, M.G. Tozzi, *Frontiers in Pharmacology*, 12 (2021).
[27] C. Ronco, S. Rocchi, R. Benhida, *Mediastinum*, 2 (2018) 26–26.
[28] H.M. Berman, *Nucleic Acids Research*, 28 (2000) 235–242.
[29] S. Kim, P.A. Thiessen, E.E. Bolton, J. Chen, G. Fu, A. Gindulyte, L. Han, J. He, S. He, B.A. Shoemaker, J. Wang, B. Yu, J. Zhang, S.H. Bryant, *Nucleic Acids Research*, 44 (2015) 1202–1213.
[30] C. Yang, E.A. Chen, Y. Zhang, *Molecules*, 27 (2022) 4568.
[31] S. Pawar, C. Kulkarni, Puja Gadade, Supriya Pujari, Surajkumar Kakade, S.H. Rohane, V.K. Redasani, *Asian Journal of Pharmaceutical Research*, 13 (2023) 292–296.
[32] Y. Wang, C.S. Lupala, H. Liu, X. Lin, *Current Topics in Medicinal Chemistry*, 18 (2019) 2268–2277.
[33] H. Li, F.N. Musayev, J. Yang, J. Su, Q. Liu, W. Wang, X. Fang, Z. Liu, Q. Liu, *Protein Science*, 31 (2021) 797–810.
[34] G. Kurisu, *Journal of Biochemistry*, 171 (2022) 3–11.
[35] N.M. O'Boyle, M. Banck, C.A. James, C. Morley, T. Vandermeersch, G.R. Hutchison, *Journal of Cheminformatics*, 3 (2011) 1-14.
[36] D.S. Goodsell, M.F. Sanner, A.J. Olson, S. Forli, *Protein Science*, 30 (2020) 31–43.
[37] G.M. Morris, R. Huey, A.J. Olson, *Current Protocols in Bioinformatics*, 24 (2008) 8-14.
[38] J. Eberhardt, D. Santos-Martins, A.F. Tillack, S. Forli, *Journal of Chemical Information and Modeling*, 61 (2021) 3891-3898.
[39] R.E. Rigsby, A.B. Parker, *Biochemistry and Molecular Biology Education*, 44 (2016) 433–437.
[40] S. Salentin, S. Schreiber, V.J. Haupt, M.F. Adasme, M. Schroeder, *Nucleic Acids Research*, 43 (2015) 443–447.
[41] M.F. Adasme, K.L. Linnemann, S.N. Bolz, F. Kaiser, S. Salentin, V.J. Haupt, M. Schroeder, *Nucleic Acids Research*, 49 (2021) 530–534.
[42] R. Fährrolfes, S. Bietz, F. Flachsenberg, A. Meyder, E. Nittinger, T. Otto, A. Volkamer, M. Rarey, *Nucleic Acids Research*, 45 (2017) 337–343.
[43] S. Jo, T. Kim, V.G. Iyer, W. Im, *Journal of Computational Chemistry*, 29 (2008) 1859–1865.
[44] J. Lee, X. Cheng, J.M. Swails, M.S. Yeom, P.K. Eastman, J.A. Lemkul, S. Wei, J. Buckner, J.C. Jeong, Y. Qi, S. Jo, V.S. Pande, D.A. Case, C.L. Brooks, A.D. MacKerell, J.B. Klauda, W. Im, *Journal of Chemical Theory and Computation*, 12 (2015) 405–413.
[45] D. Van Der Spoel, E. Lindahl, B. Hess, G. Groenhof, A.E. Mark, H.J.C. Berendsen, *Journal of Computational Chemistry*, 26 (2005) 1701–1718.
[46] W. Humphrey, A. Dalke, K. Schulten, *Journal of Molecular Graphics* ,14 (1996) 33–38.
[47] M.S. Valdés-Tresanco, M.E. Valdés-Tresanco, P.A. Valiente, E. Moreno, *Journal of Chemical Theory and Computation*, 17 (2021) 6281–6291.
[48] B.R. Miller, T.D. McGee, J.M. Swails, N. Homeyer, H. Gohlke, A.E. Roitberg, *Journal of Chemical Theory and Computation*, 8 (2012) 3314–3321.
[49] S. Genheden, U. Ryde, *Expert Opinion on Drug Discovery*, 10 (2015) 449–461.
[50] E. Wang, G. Weng, H. Sun, H. Du, F. Zhu, F. Chen, Z. Wang, T. Hou, *Physical Chemistry Chemical Physics*, 21 (2019) 18958–18969.